Lithos 126 (2011) 127–134

Contents lists available at ScienceDirect

Lithos

journal homepage: www.elsevier.com/locate/lithos

Precisely dating Paleozoic kimberlites in the North China Craton and Hf isotopic constraints on the evolution of the subcontinental lithospheric mantle

Qiu-Li Li [a,*], Fu-Yuan Wu [a], Xian-Hua Li [a], Zhi-Li Qiu [b], Yu Liu [a], Yue-Heng Yang [a], Guo-Qiang Tang [a]

[a] State Key Laboratory of Lithospheric Evolution, Institute of Geology and Geophysics, Chinese Academy of Sciences, Beijing 100029, China
[b] Department of Earth Sciences, Sun Yat-Sen University, Guangzhou 510275, China

ARTICLE INFO

Article history:
Received 16 March 2011
Accepted 6 July 2011
Available online 19 July 2011

Keywords:
Kimberlite
North China Craton
Baddeleyite
Hf isotope
Subcontinental lithospheric mantle

ABSTRACT

Kimberlite, a deep-sourced ultramafic potassic rock, carries not only diamond, but also invaluable mantle xenoliths and/or xenocrysts, which are important for tracking the evolution of subcontinental lithospheric mantle (SCLM). However, it is challenging to accurately determine the emplacement age of kimberlite and its compositions of primary magma because of modifications by crustal and/or mantle contamination and post-emplacement alteration. This paper reports emplacement ages of diamondiferous kimberlites in Mengyin and Fuxian of the North China Craton (NCC) using three different dating methods. For Mengyin kimberlite, single-grain phlogopite Rb–Sr dating yields an isochron age of 485 ± 4 Ma, U–Th–Pb analyses on perovskite give a ^{238}U–^{206}Pb age of 480.6 ± 2.9 Ma and a ^{232}Th–^{208}Pb age of 478.9 ± 3.9 Ma, and baddeleyite yields a ^{207}Pb–^{206}Pb age of 480.4 ± 3.9 Ma. For Fuxian kimberlite, baddeleyite gives a ^{207}Pb–^{206}Pb age of 479.6 ± 3.9 Ma, indicating that the Paleozoic kimberlites in the NCC were emplaced at ~480 Ma. Numerous lines of evidence indicate that the studied baddeleyites are xenocrysts from the SCLM, and can be used to constrain Hf isotope compositions ($\varepsilon_{Hf}(t) \sim -6$) of the SCLM when kimberlite erupted. Combined with data from Mesozoic–Cenozoic mantle-derived rocks and xenoliths, the Hf isotope evolution trend of the SCLM beneath NCC before craton destruction was tentatively constructed, which suggested that the Archean SLCM was enriched by metasomatism at ~1.3 Ga. Further Hf isotope investigations on additional SCLM-derived materials could be used to compare with the constructed Hf isotope evolution trend before craton destruction to determine when lithospheric thinning occurred.

1. Introduction

The North China Craton (NCC) (Fig. 1) is one of the world's oldest Archean blocks as manifested by crustal remnants as old as 3800 Ma (Liu et al., 1992; Song et al., 1996; Wu et al., 2008a; Zheng et al., 2004a). The existence of Ordovician diamondiferous kimberlites in the NCC indicates a thick (~200 km) lithosphere in the early Paleozoic. However, at present the lithosphere is < 80 km thick as revealed by seismic studies and petrologic studies of mantle xenoliths in Mesozoic–Cenozoic "intra-plate" volcanism, suggesting that a significant part of the original lithospheric mantle beneath the eastern NCC was removed during the Phanerozoic (e.g. Fan and Menzies, 1992; Gao et al., 2002; Griffin et al., 1998; Menzies et al., 1993, 2007; Menzies and Xu, 1998; Xu, 2001; Zheng et al., 1998, 2007). The thick, old, cold and refractory subcontinental lithospheric mantle (SCLM) beneath the NCC was subsequently replaced by thin, young, hot and fertile mantle (e.g. Gao et al., 2002; Griffin et al., 1998; Huang et al., 2007; Menzies and Xu, 1998; Menzies et al., 2007; Wu et al., 2003, 2006a; Xu, 2001; Zhang et al., 2008; Zheng et al., 1998).

Although extensive investigations have been conducted on the lithospheric thinning process, there are still considerable debate on its mechanism, with lithospheric delamination (e.g. Deng et al., 2007; Gao et al., 2002, 2004, 2008; Wu et al., 2003, 2005a) and thermo-mechanical erosion (e.g.Griffin et al., 1998; Menzies and Xu, 1998; Xu, 2001; Zhang, 2005; Zhang et al., 2008) being commonly proposed. The delamination model, (a more rapid process), proposes that the thinning was triggered by foundering and sinking of heavy material, and predicts that the present SCLM is juvenile. In contrast, the erosion model emphasizes a slow chemical process of asthenospheric upwelling, forming a stratified SCLM with Archean relict overlying newly accreted material (Griffin et al., 1998; Menzies and Xu, 1998).

Understanding SCLM evolution is helpful in deciphering the lithospheric thinning mechanisms. For this reason, extensive studies have been conducted on mantle xenoliths and SCLM-derived mafic-alkaline rocks in the NCC (e.g., Chu et al., 2009; Gao et al., 2002; Wu et al., 2003, 2006a; Xu et al., 2008; Zhang et al., 2008; Zheng et al., 2009). However, our knowledge about the Paleozoic SCLM beneath the NCC is rather limited. Firstly, the age of the diamondiferous Mengyin (Shandong province) and Fuxian (Liaoning Province) kimberlites, erupted on opposite sides of the translithospheric Tanlu fault (Fig. 1), is not well determined. Available geochronological data yield a wide range from

* Corresponding author. Tel.: +86 10 82998443; fax: +86 10 62010846.
E-mail address: liqiuli@mail.iggcas.ac.cn (Q.-L. Li).

0024-4937/$ – see front matter © 2011 Published by Elsevier B.V.
doi:10.1016/j.lithos.2011.07.001

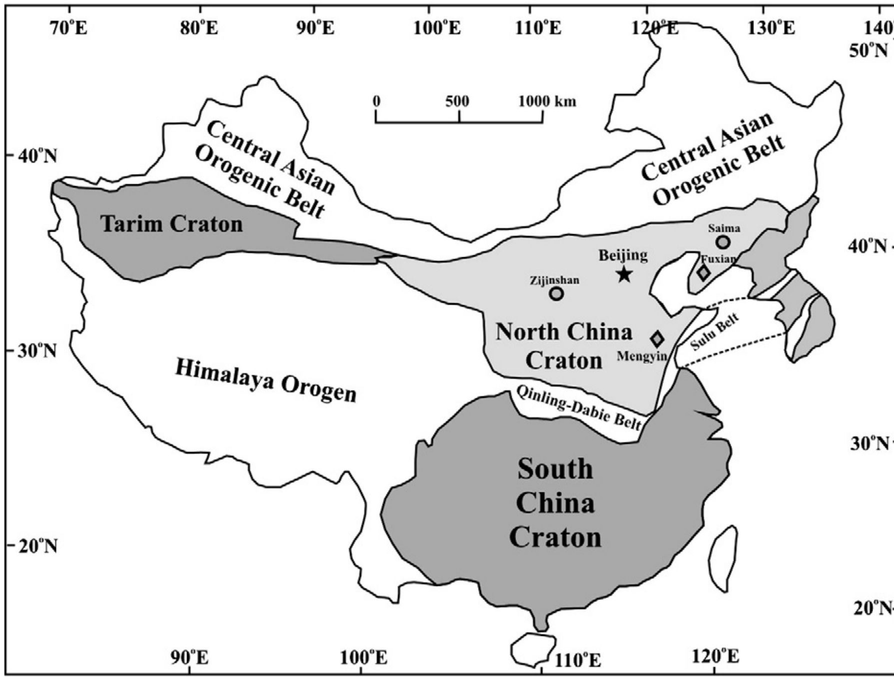

Fig. 1. Geological sketch map showing the Cratons in China and sample localities discussed in the text. Diamond: kimberlite. Circle: nepheline syenite.

456 Ma to 475 Ma based on phlogopite Rb–Sr and Ar–Ar, perovskite U–Pb by TIMS and LA-ICPMS methods (Dobbs et al., 1994; Li et al., 2005; Yang et al., 2009; Zhang and Yang, 2007). Secondly, although it has been proposed that the Paleozoic SCLM was Sr–Nd isotopically enriched, significantly different from that of depleted SCLM in the Cenozoic (Chi and Lu, 1996; Fan and Menzies, 1992; Griffin et al., 1998; Huang et al., 2007; Menzies and Xu, 1998; Zheng et al., 1998), this conclusion was based on the limited data from significantly altered peridotite samples. The Os isotope character of these altered samples is likely to be less disturbed and so an Archean melt-extraction age can be established (Chu et al., 2009; Gao et al., 2002; Wu et al., 2006a; Zhang et al., 2008; Rudnick et al., 2004), however other isotopic features like Sr–Nd–Hf systems of the SCLM are still in doubt or remain unknown (Wu et al., 2008b).

In this paper, we report a series of comprehensive dating results of phlogopite Rb–Sr, perovskite ^{238}U–^{206}Pb and ^{232}Th–^{208}Pb and baddeleyite ^{207}Pb–^{206}Pb analyses obtained from the Mengyin and Fuxian kimberlites. The baddeleyites, considered to be mantle xenocrysts, were used to trace the Hf isotope composition of the Paleozoic SCLM.

2. Geological settings and samples

The NCC is the oldest tectonic unit in China, with crustal components up to ca. 3.8 Ga exposed in the far north-east (e.g., Liu et al., 1992; Wu et al., 2008a). The Early Paleozoic Qilianshan Orogen and the Late Paleozoic Central Asian Orogenic Belt bound the craton to the west and the north, respectively, and in the south the Qinling-Dabie-Sulu ultrahigh-pressure metamorphic belt separates it from the South China Craton (Fig. 1). Based on age, lithological assemblage, tectonic evolution and P–T–t paths, the NCC has been divided into Eastern and Western blocks, which were amalgamated along the Paleoproterozoic Trans-North China Orogen (Zhao et al., 2005 and references therein). Based on today's seismology and geography, the NCC can be separated into two different tectonic domains by the N–S trending Daxinganling–Taihangshan gravity lineament (DTGL) (Ma, 1989; Menzies and Xu, 1998).

Similar to other Archean blocks around the world, the NCC contains both greenstone belts and high-grade metamorphic terrains, which were metamorphosed at 2.5 Ga and subsequently cratonized at 1.8 Ga by collision of the Eastern and Western blocks (e.g., Wu et al., 2005a; Zhao et al., 2005). After 1.8 Ga, the NCC has remained relatively stable and was covered by a thick sequence of Mesoproterozoic to Paleozoic sediments. In the Paleozoic, when the diamondiferous Mengyin and Fuxian kimberlites were emplaced in Shandong and Liaoning provinces, respectively (Zhang et al., 1989), and the NCC was characterized by thick carbonate sedimentation during the Cambrian to Early Ordovician. In the Mesozoic, extensive volcanic activity and granitoid emplacement occurred in the eastern NCC, possibly due to the interaction of the Eurasian and Pacific plates and resulting from the lithospheric thinning (Wu et al., 2003, 2005b). During the Cenozoic, numerous alkaline basalts containing mantle peridotite and minor lower-crustal granulites xenoliths were erupted throughout the central and eastern parts of the craton.

In this study, kimberlites from Mengyin and Fuxian were investigated. The Mengyin kimberlites are diamondiferous and erupted through the Archean Taishan Complex. About 100 kimberlitic dykes and pipes have been identified (Fig. 1, Chi and Lu, 1996; Wan, 1989). Among them, the pipe 1 (Shengli 1, N35°40′ and E117°47′) is the most important diamondiferous one in the area and was targeted for this study. Perovskite is relatively abundant in the Mengyin kimberlite groundmass, with concentrations up to 5% (rarely up to 20%, Yang et al., 2009). Most perovskite grains are dark orange to brown and euhedral shapes with grain sizes ranging from 30 to 200 μm. Phlogopite and perovskite were separated from sample MY12, the only one containing baddeleyite, for further investigation. The Fuxian diamondiferous kimberlites are emplaced in the Mesoproterozoic–Cambrian country rocks (Fig. 1). Samples here show more extensive alteration and weathering. Although a number of kimberlite samples were used to separate perovskite and baddeleyite, perovskite is extremely rare and baddeleyite was obtained from only one rock sample. In both localities, these kimberlites contain a variety of crustal fragments, including limestone, gneiss, amphibolite, mafic granulite xenoliths (Chi and Lu, 1996; Dong, 1994; Wan, 1989; Zheng et al., 2004a,b) and exotic zircons with ages of 2.5 Ga (Yin et al., 2005; Zheng et al., 2009).

3. Analytical procedures

The kimberlite samples were crushed using a jaw crusher and bico disk mill equipped with hardened steel plates. Minerals were concentrated using a wilfley Table, heavy liquids and a Frantz

Isodynamic separator. Clean and fresh mineral grains were hand-picked under a binocular microscope. Minerals fractions including phlogopite, baddeleyite and perovskite were separated from sample MY12 of the Mengyin kimberlite, and baddeleyite from sample FX-1 of the Fuxian kimberlite. Phlogopite grains were selected for single-grain Rb–Sr dating, and perovskites were analyzed for U–Pb dating, whereas baddeleyites were selected for U–Pb or Pb–Pb dating and Hf isotope analyses. All analyses were performed at the Institute of Geology and Geophysics, Chinese Academy of Sciences (IGGCAS) and are detailed in Electronic Appendix file.

4. Analytical results

4.1. Phlogopite Rb–Sr age

Single-grain phlogopite Rb–Sr isotopic data for the MY12 kimberlite sample after blank and spike corrections are shown in Fig. 2 and Appendix Table 1. Regression and age calculation of isochron were performed using the Isoplot software (Ludwig, 2003). The decay constant of ^{87}Rb is 1.42×10^{-11} as recommended by Steiger and Jäger (1977), giving 1.5% for errors of ^{87}Rb/^{86}Sr ratios and 0.01% for errors of ^{87}Sr/^{86}Sr ratios. Rb and Sr contents were calculated using estimated weight of the analyzed grains (ca. 0.1 mg per grain). Eight individual grains of phlogopite give ^{87}Rb/^{86}Sr ranging from 18.6 to 450 and yield an isochron age of 485 ± 4 Ma with an initial ^{87}Sr/^{86}Sr of 0.7138 ± 0.0029 (MSWD = 0.5, Fig. 2a).

For a comparison, Rb–Sr isochron of the Fuxian phlogopite measured in Li et al. (2005) is also shown here (Fig. 2b). Eleven analyses yielded an age of 463 ± 7 Ma with an initial ^{87}Sr/^{86}Sr of 0.7225 ± 0.0057. This age is ~20 Ma younger than that obtained for the Mengyin phlogopite. The Fuxian phlogopites have higher initial Sr isotopic ratio than the Mengyin samples.

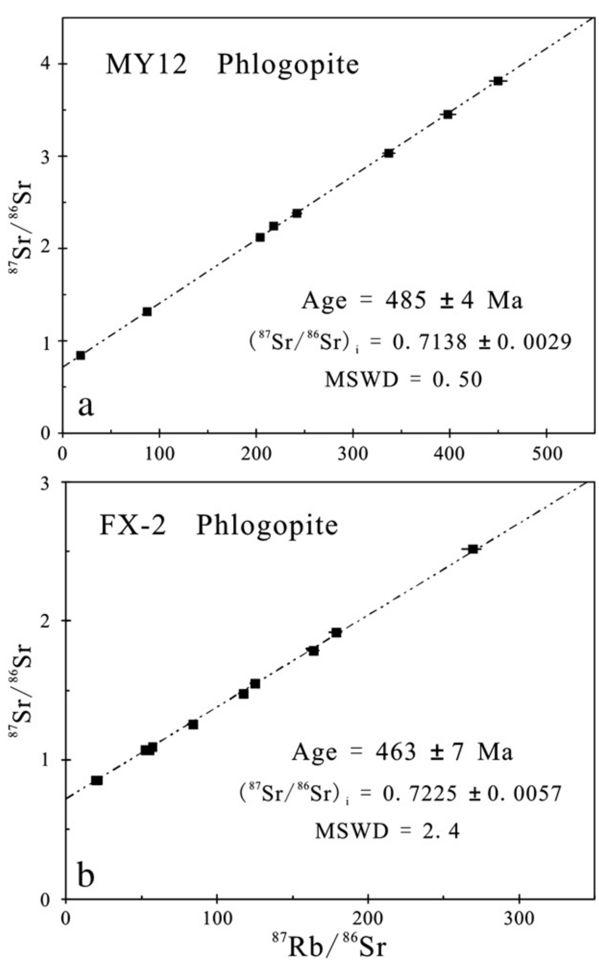

Fig. 2. Single-grain phlogopite Rb–Sr isochrons of the Mengyin kimberlite (a) and Fuxian kimberlite (b).

4.2. Perovskite U–Th–Pb ages

MY12 perovskites are euhedral and fresh with grain sizes ranging from 30 to 100 μm (Yang et al., 2009). Fifteen U–Pb analyses were performed in separated two sessions. The data are plotted in Fig. 3 (Appendix Table 2). All the 30 analyses show that MY12 perovskites are fairly homogeneous with a uranium content of 72 ± 7 ppm (1 SD). Common lead ranges from 5 to 11 ppm, and the ^{204}Pb-based f_{206} value (percentage of common lead ^{206}Pb in total ^{206}Pb) ranges from 22% to 26%. Thorium content varies significantly, with Th/U ranging from 22 to 106. Due to the tight clustering of data points, a Tera–Wasserburg plot gave an imprecise lower intercept age at 501 ± 55 Ma, and an imprecise upper intercept of common ^{207}Pb/^{206}Pb composition at 0.94 ± 0.19 as well. However, if the terrestrial Pb model of Stacey and Kramers (1975) is applied as an estimate of common lead composition, a Concordia U–Pb age of 480.6 ± 2.9 Ma can be obtained (Fig. 3). A weighted average ^{206}Pb/^{238}U age derived by the ^{204}Pb-based common-Pb correction is 480.9 ± 2.8 Ma (MSWD = 1.0), identical to the average ^{206}Pb/^{238}U age of 480.9 ± 2.5 Ma (MSWD = 1.1) given by the ^{207}Pb-based common-Pb correction. The rather high Th contents result in low ^{204}Pb-based f_{208} values (percentage of common lead ^{208}Pb in total ^{208}Pb) ranging from 2.3% to 6.8%. A weighted average of ^{208}Pb/^{232}Th ages is 478.9 ± 3.9 Ma (MSWD = 0.49, Fig. 3, inserted). The agreement between the ^{238}U–^{206}Pb and ^{232}Th–^{208}Pb ages indicates a closed U–Th–Pb system in this perovskite (Li et al., 2010b).

4.3. Baddeleyite U–Pb and Pb/Pb ages

Baddeleyite grains from MY12 kimberlite are subhedral or fragmental with 10–100 μm in length (Fig. 4a). Nineteen Pb/Pb analytical data with multi-collector mode are listed in Appendix Table 3 and plotted in Fig. 4b. Uranium contents range from 84 to 467 ppm. Their measured radiogenic ^{207}Pb/^{206}Pb are indistinguishable within analytical errors, with a weighted mean of 0.05671 ± 0.00010, corresponding to a Pb/Pb age of 480.4 ± 3.9 Ma (MSWD = 0.91, Fig. 4b).

Like the Mengyin kimberlite, baddeleyite grains from Fuxian kimberlite (sample FX-1) are also subhedral and fragmental, and are 10–100 μm in length (Fig. 4c). Twenty five U–Pb analyses were conducted under mono-collector mode and the data are reported in Appendix Table 4, and the obtained Pb/Pb age is shown in Fig. 4d. It is noted that the FX-1 baddeleyites contain high and variable U content from 628 to 2958 ppm, and many grains show extremely high Th contents (up to 1328 ppm) with Th/U up to 0.45. The calculated U–Pb ages are variable between 443 and 550 Ma and broadly positively correlate with U, Th contents and Th/U, which could be attributed to crystal orientation effect (Wingate and Compston, 2000) and/or high U effect (Li et al., 2010a; Williams and Hergt, 2000). However, radiogenic ^{207}Pb/^{206}Pb of 25 measurements are consistent, within analytical errors, with a weighted average of 0.05669 ± 0.00013, corresponding to a Pb/Pb age of 479.6 ± 4.9 Ma (MSWD = 0.71, Fig. 4d).

4.4. Baddeleyite Hf isotope compositions

The Hf analyses were obtained using the same mounts which were previously used for U–Pb and Pb–Pb dating. The results are shown in Fig. 5 and Appendix Table 5. All baddeleyites have very low ^{176}Lu/^{177}Hf (0.000005–0.000033). However, the small grain size, mostly < 30 μm in width, and needle- to wafer-shaped morphology make the laser-ablation measurements quite difficult. Many grains were ejected after short bombardment of laser, which resulted in big errors. Nevertheless, twenty-eight analyses on MY12 baddeleyite were obtained with internal uncertainty ranging from 0.000031 to 0.000079 at $2\sigma_m$ level. Though all measured $^{176}Hf/^{177}Hf$ ratios show a Gaussian distribution pattern (Fig. 5a), those data with internal uncertainty larger than 0.00005 were excluded to calculate the average. A weighted average of $^{176}Hf/^{177}Hf$ is 0.282286 ± 0.000020 ($2\sigma_m$, n = 12, MSWD = 2.5), corresponding to ε_{Hf} (t = 480 Ma) value of −6.62 ± 0.64 (Fig. 5a).

Nineteen measurements on FX-1 baddeleyite show variations of $^{176}Hf/^{177}Hf$ ranging from 0.282283 to 0.282389 with internal uncertainties from 0.000014 to 0.000035 at $2\sigma_m$ level. Similarly, the Hf isotopic data show a single population, and have a weighted average value of 0.282308 ± 0.000010 ($2\sigma_m$, n = 18/19, MSWD = 1.6), corresponding to ε_{Hf} (t = 480 Ma) value of −5.86 ± 0.36 (Fig. 5b).

5. Discussion

5.1. Emplacement age of kimberlites

Kimberlites and related rocks are a series of volatile-rich potassic ultramafic rocks that originate from the deep lithospheric or sub-lithospheric mantle (Mitchell, 1986, 1995; Woolley et al., 1996). They generally contain abundant crustal and mantle xenoliths and are highly susceptible to alteration and weathering. Therefore, the combined effects of contamination and post-emplacement alteration make it difficult not only for determining the compositions of the primary kimberlite magmas, but also the age of their emplacement (Heaman, 1989; Li et al., 2010b; Mitchell, 1986).

There have been several attempts to date the emplacement age of the Mengyin kimberlite. A Rb–Sr isotopic analysis of phlogopite yielded an isochron age of 475 ± 3 Ma (Dobbs et al., 1994), broadly consistent with our single-grain phlogopite Rb–Sr result of 485 ± 4 Ma in this study. However, the initial $^{87}Sr/^{86}Sr$ (I_{Sr}) of the analyzed phlogopites lie between 0.704 and 0.714 (Dobbs et al., 1994; this study), variably higher than that of perovskite (0.7037 from Yang et al., 2009), suggesting a significant crustal contamination and/or later alteration. In addition to the Rb–Sr technique, Ar–Ar analyses of phlogopite were also used to date kimberlite, which yielded an age of 465 ± 3 Ma for the Mengyin kimberlite (Zhang and Yang, 2007), ~15 Ma younger than the result of the Rb–Sr isochron. The Ar–Ar age spectrum, however, indicates mixture of different mineral phases and/or partial Ar loss (Zhang and Yang, 2007).

Perovskite is considered as a good mineral for dating kimberlite because it has high U content, occurs mainly in the kimberlite groundmass and is considered to have crystallized during the early stages of the magmatic history (e.g. Batumike et al., 2008; Kinny et al., 1997; Kramers and Smith, 1983; Yang et al., 2009). Unfortunately, some perovskites in the Mengyin kimberlite suffered different levels of alteration, and hence variable radiogenic Pb loss (Yang et al., 2009). It is also noteworthy that perovskite usually contains a high proportion of common lead, which makes it difficult to judge the concordance of U–Pb system. In this case, only an apparent $^{206}Pb/^{238}U$ age can be obtained. Previous ^{238}U–^{206}Pb perovskite ages of 456 ± 8 Ma obtained by TIMS (Dobbs et al., 1994) and 470 ± 4 Ma by LA-ICPMS (Yang et al., 2009) can also be attributed to the alteration. In our work, perovskite was analyzed by ion probe which consumed only a small volume of sample on the least alterated part (judged by BSE images) of the mineral interior. Our consistent ^{238}U–^{206}Pb and ^{232}Th–^{208}Pb ages demonstrate that the dated Mengyin perovskites should be concordant in U–Th–Pb system (Li et al., 2010b). Therefore, perovskites U–Th–Pb age of 480 ± 4 Ma is suggested as the best estimate of the emplacement age of the Mengyin kimberlite. Baddeleyites from the Mengyin kimberlite yielded a Pb–Pb age of 480.4 ± 3.9 Ma, which is in good agreement with perovskite U–Th–Pb ages. As discussed below, the studied baddeleyite may be inherited from the mantle source, but its U–Pb analyses can provide age estimation for kimberlite as some kimberlitic zircons (Belousova et al., 2001; Davis et al., 1976; Kinny et al., 1989).

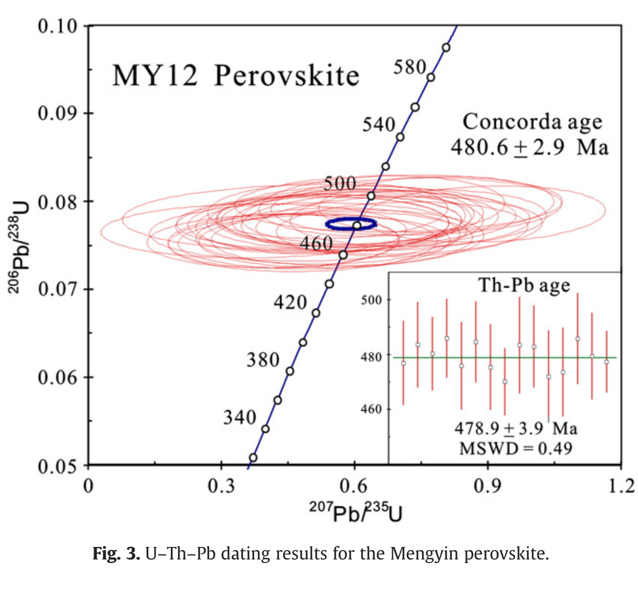

Fig. 3. U–Th–Pb dating results for the Mengyin perovskite.

As for the Fuxian kimberlite, while the phlogopite Ar–Ar plateau date of 464 ± 2 Ma (Zhang and Yang, 2007) is consistent with previously reported Rb–Sr isochron dates of ~463 Ma (Dobbs et al., 1994; Li et al., 2005), mixture of different mineral phases and/or partial Ar loss was noticed (Zhang and Yang, 2007). In addition, the initial $^{87}Sr/^{86}Sr$ values (I_{Sr}) of 0.722 from phlogopite Rb–Sr isochron regression (Fig. 2b) is much higher than those of the mantle-derived magmas, indicating significant crustal contamination and/or later alteration. Therefore, both the Rb–Sr and Ar–Ar ages are likely to be questionable. Unfortunately, despite repeated attempts separation of perovskite from the Fuxian kimberlite was unsuccessful. However, baddeleyite from one sample yielded a Pb/Pb age of 479.6 ± 3.9 Ma. Based on the concordance of the perovskite U–Th–Pb age and the baddeleyite Pb/Pb age from the Mengyin kimberlite, this baddeleyite Pb/Pb age is interpreted as the age of emplacement of the Fuxian kimberlite.

Comparison with the aforementioned different isotopic systems suggests that phlogopite is not an ideal mineral for dating the kimberlite by Rb–Sr and Ar–Ar methods because of its complicated alteration and/or contamination processes. Although dating baddeleyite can yield the precise crystallization age of a kimberlite, it is rarely found in kimberlites and could be xenocrystic in origin (see discussion below). Perovskite in the kimberlite groundmass is therefore thought to be the best candidate to date kimberlite, particularly using the ion probe technique that can effectively avoid alteration in some crystals (Yang et al., 2009). More importantly, simultaneous measurement of the perovskite U–Pb and Th–Pb age makes it possible to determine the concordance of U–Th–Pb system of the mineral, thus providing a robust constraint on the emplacement age of kimberlite (Li et al., 2010b).

5.2. Xenocrystic origin of kimberlitic baddeleyite

Baddeleyite rarely occurs in kimberlite (Mitchell, 1986). Two distinct types of baddeleyite can be recognized from this kind of rocks (Heaman and LeCheminant, 1993 and reference therein). The first baddeleyite type occurs as a rim on zircon megacrysts or sometimes interfaces between zircon and rutile/ilmenite, which is interpreted as products formed by reaction between macrocrystal zircon and kimberlite melt undersaturated in SiO_2 and enriched in carbonate component. In fact, this type of baddeleyite forms fine idiomorphic crystals which are mostly oriented perpendicular to contours of zircon grains and they are often parallel to each other. Crystals show a zoned structure, but commonly have dark central parts and light marginal parts in back-scattered electron images, indicating a higher U content in rim than core (Heaman and LeCheminant, 1993). The second type of baddeleyite occurs as xenocrysts, as documented in Mbuji–Mayi kimberlite and ˆIle Bizard alnöite (Heaman and LeCheminant, 2000; Schärer et al., 1997). In this case, the baddeleyite was originally formed in the mantle and then picked up by the deep-sourced magma. No matter how these baddeleyites formed, this mineral has been proven to record the emplacement age of magmas as its U–Pb isotopic clock was triggered while being caught by the mantle-derived magmas (Heaman and LeCheminant, 1993, 2000; Schärer et al., 1997).

Several lines of evidence support the xenocrystic origin for baddeleyites from the Mengyin and Fuxian kimberlites. Firstly, baddeleyite is very rare and can only be obtained occasionally. It is much easier to obtain crustal zircon xenocrysts than baddeleyites. We have not found any evidence showing reactions between xenocrystic zircon and kimberlite melt. Secondly, the CL images of the Mengyin and Fuxian baddeleyites show zoning, but commonly suggesting higher U content in core than rim, contrary to what formed by reaction between macrocrystic zircon and kimberlite melt (Heaman and LeCheminant, 1993). No zircon exists as residue in the core. Thirdly, the studied baddeleyite grains, although fragmental, have a grain size of >50 μm (Fig. 4), much bigger than the crystallized baddeleyite from kimberlitic magma (Mitchell, 1986). Fourthly, the ε_{Hf} (480 Ma) value of ca. –6 for baddeleyites is different from not only that of the kimberlite magma (−0.3 to −6, Zhang and Yang, 2007), but also the xenocrystic zircons (ca. −40, Zheng et al., 2009). This clearly indicates that baddeleyites did not crystallize from the kimberlitic magma or were assimilated from crustal rocks.

In summary, the baddeleyites from the Mengyin and Fuxian kimberlites are most likely xenocrysts from the SCLM. These crystals formed either directly from a melt by metasomatism, or through subsolidus crystallization (Schärer et al., 1997) and stayed in the lithospheric mantle at high temperature with U–Pb isotopic system remaining open. After eruption, its U–Pb systems were closed due to cooling and crystallization of kimberlitic magma. Therefore, these xenocrystic baddeleyites record the emplacement age of kimberlite.

As for Hf isotope composition, with the exception of those measurements with large uncertainties, baddeleyites from Mengyin and Fuxian kimberlites show a narrow range of ±2 ε_{Hf} units, which is close to the external precision of the analytical method (Wu et al., 2006b). This narrow range of ε_{Hf} values might be consistent with crystallization from a single magma that was in equilibrium with the Hf composition of the SCLM (Griffin et al., 2000). Their Hf model age points to ~1.3 Ga, which may record a metasomatism event manifested by the widespread ~1.35 Ga diabase intrusion event in the NCC (Zhang et al., 2009).

5.3. Evolution of the SCLM of NCC

Based on Os isotope characteristics and high Fo number of olivine in peridotite xenoliths from Mengyin and Fuxian kimberlite, it is believed that the lithospheric mantle keel of NCC had an Archean melt-extraction age (e.g., Chu et al., 2009; Gao et al., 2002; Wu et al., 2003, 2006a; Zhang et al., 2008; Zheng et al., 2006). In contrast, geophysical observations and geochemical characteristics of peridotite xenoliths transported by Cenozoic basalts indicate the current SCLM beneath the eastern NCC is thin, hot and fertile (e.g. Griffin et al., 1998; Zheng et al., 2006). This contrast suggests that ~100 km of cratonic lithosphere had been removed between early Ordovician and Cenozoic, and the refractory and isotopically enriched SCLM had been changed to be fertile and isotopically depleted. However, the mechanisms and processes of this lithospheric thinning and mantle transformation have been hotly

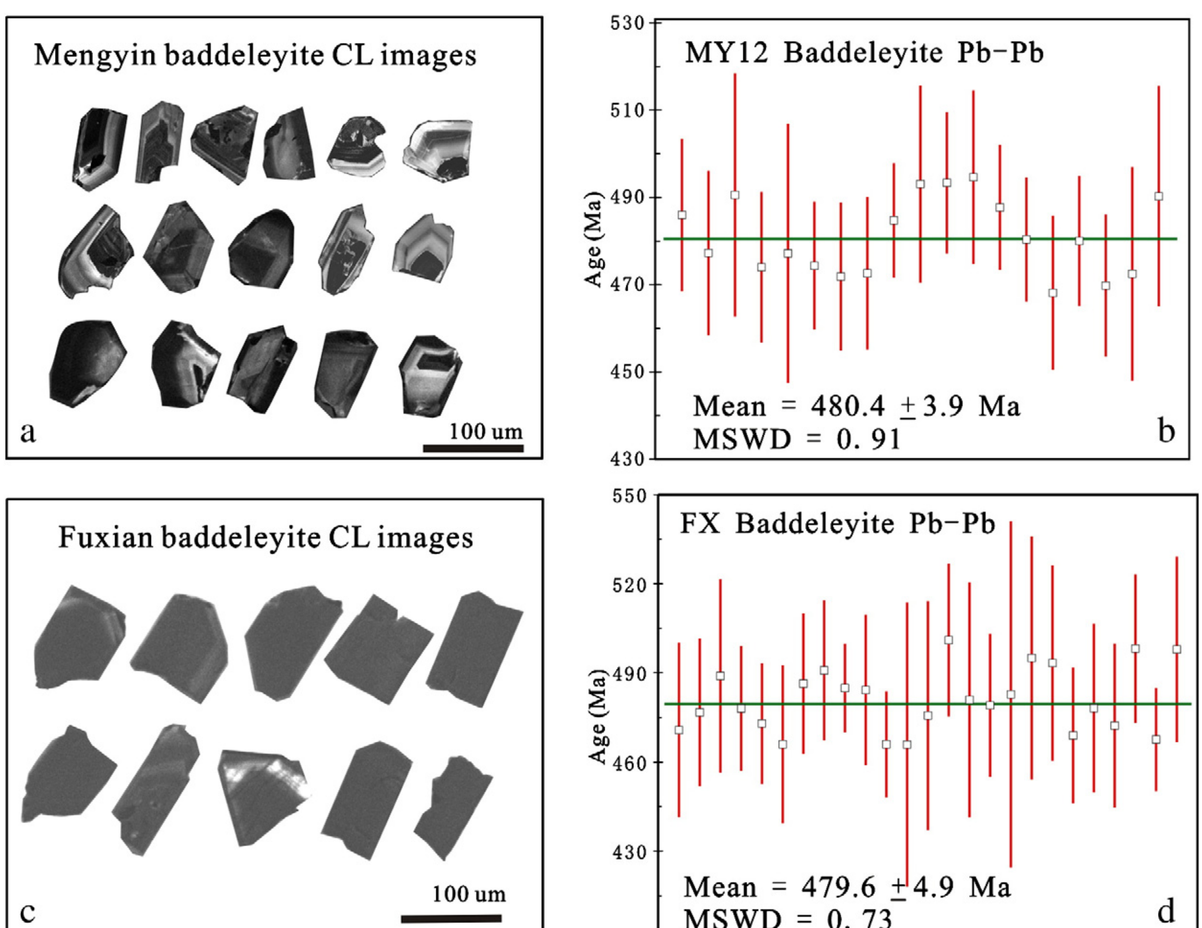

Fig. 4. CL images and Pb/Pb ages of baddeleyite xenocrysts from kimberlites of Mengyin (a,b) and Fuxian (c,d).

debated during last decade. Obviously, to investigate how and when the craton was destroyed requires detailed physical–chemical knowledge of the original SCLM before destruction.

The deep-sourced magmas and trapped mantle xenoliths and xenocrysts provide critical information of both the chemical composition and evolution of the SCLM. Extensive studies have been conducted on mantle xenoliths and SCLM-derived mafic-alkaline rocks in the NCC (e.g., Chu et al., 2009; Gao et al., 2002; Huang et al., 2007; Qiu et al., 2005; Wu et al., 2003, 2006a; 2010; Xu et al., 2008; Ying et al., 2007; Zhang et al., 2008; Zheng et al., 2006, 2009). However, it is not known if the Paleozoic SCLM beneath the NCC was isotopically enriched or depleted since the intensive alteration makes impossible to obtain reliable isotopic compositions of the peridotite xenoliths in the Paleozoic kimberlites. It is noted that, despite many studies on the Mesozoic mantle-derived rocks, crustal contamination during crystallization similarly makes them unreliable in constraining the characteristics of the SCLM, and so only those SCLM-derived igneous rocks with little crustal contamination can provide reliable information. Fortunately, silica undersaturated nepheline syenite, although rare in the NCC, can provide useful data on the SCLM evolution in the NCC.

One important nepheline syenite is the Triassic (~225 Ma) Saima complex in the Liaodong Peninsula of northern China (Fig. 1). It is composed of an eastern syenite, central alkaline volcanic rocks (trachyte, leucite phonolite and syenitic porphyry), and western nepheline syenite (Wu et al., 2010 and references therein). It has been well documented that this nepheline syenite has fairly homogeneous Hf isotope composition of $^{176}Hf/^{177}Hf = \sim 0.282330$, corresponding to $\varepsilon_{Hf}(t) \sim -11$ (Wu et al., 2010). Another nepheline syenite is the Cretaceous (~127 Ma) Zijinshan complex, located in western NCC where a thick

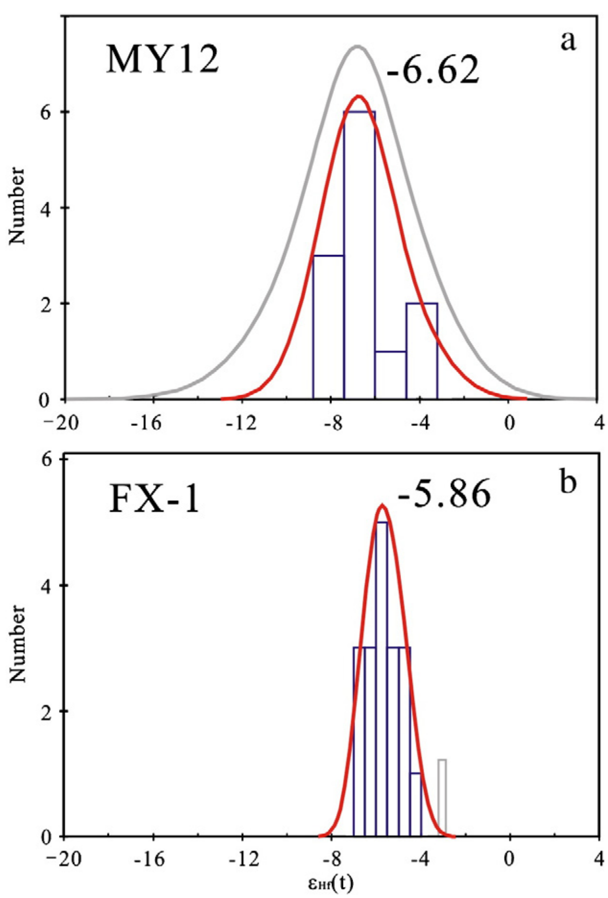

Fig. 5. Hf isotope compositions of baddeleyite xenocrysts from kimberlites of Mengyin (a) and Fuxian (b). The grey line in (a) is from all the Hf isotope analyses from baddeleyites of Mengyin kimberlite, and dark line is from those Hf isotope data with internal uncertainty less than 0.00005 ($2\sigma_m$).

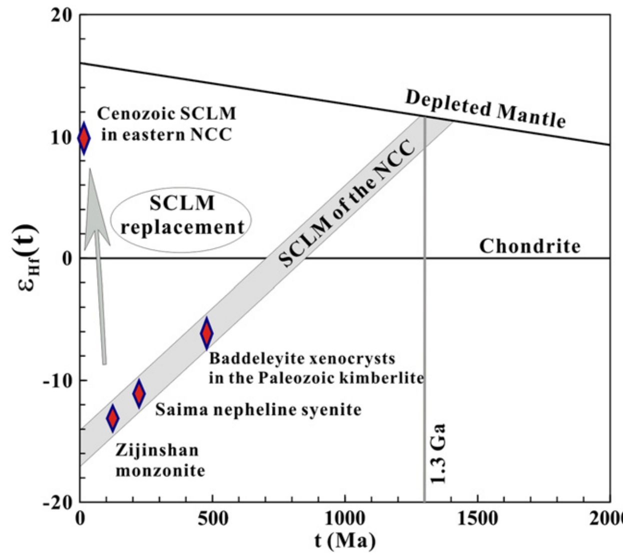

Fig. 6. Hf isotope evolution diagram of the SCLM beneath the NCC before destruction. Data source: Baddeleyite xenocrysts in the Paleozoic kimberlites (this study); Saima nepheline syenite (Wu et al., 2010); Zijinshan monzonite (Ying et al., 2007); Cenozoic SCLM in eastern NCC (Chu et al., 2009; Qiu et al., 2005).

lithospheric keel is preserved (Fig. 1). This nepheline syenite includes monzonite in its outermost part and pseudoleucite phonolitic breccia in the center. On the basis of geochemistry the monzonite has been interpreted as mixing of lithospheric mantle-derived magma with lower-crust derived melts (Ying et al., 2007). The end member of the SCLM-derived magma has a $^{176}Hf/^{177}Hf$ isotopic ratio of ~0.282335, corresponding to $\varepsilon_{Hf}(t) \sim -13$.

When all the data discussed above are plotted together (Fig. 6), it can be seen that the Hf isotopic composition of the SCLM beneath the NCC evolved in a linear trend which intersects the depleted mantle at ~1.3 Ga. This age may record a metasomatism event and it is further supported by the widespread ~1.35 Ga diabase intrusion event in the NCC (Zhang et al., 2009). This trend can be used to determine the Hf isotopic nature of the SCLM before destruction. Interestingly, the mantle xenoliths hosted in the Cenozoic basalts in eastern NCC have much higher Hf isotopic ratios (Chu et al., 2009; Qiu et al., 2005), indicating that the SCLM in the Cenozoic is juvenile, not an ancient residue. Understanding how and when this change happened calls for further Hf isotope investigations on more SCLM-derived materials to compare with the constructed Hf isotope evolution trend of the SCLM before the craton was destroyed.

6. Conclusions

We precisely determine the emplacement age of diamondiferous kimberlites from Mengyin and Fuxian in the NCC, using three different dating methods. For the Mengyin kimberlite, single-grain phlogopite Rb–Sr isochron yielded an age of 485 ± 4 Ma. U–Th–Pb analyses on perovskite gave ^{238}U–^{206}Pb age of 480.6 ± 2.9 Ma and ^{232}Th–^{208}Pb age of 478.9 ± 3.9 Ma. The baddeleyites from the Mengyin and Fuxian kimberlites yielded almost identical Pb–Pb ages of 480.4 ± 3.9 Ma and 479.6 ± 3.9 Ma, respectively, which also are best explained as the emplacement age of these kimberlites. The Hf isotope compositions (ε_{Hf} (480 Ma) = ~−6) of baddeleyite xenocrysts from these diamondiferous kimberlites have been used to probe the SCLM beneath the NCC. Combined with Hf isotopic data of the Meso-Cenozoic SCLM-derived rocks and mantle xenoliths, the Hf isotope evolution trend of the SCLM beneath the NCC before destruction was constructed, which revealed a ~1.3 Ga metasomatism event. Further Hf isotope investigations on more SCLM-derived materials could be used to compare with the constructed Hf isotope evolution trend before craton destruction to determine when the lithospheric thinning occurred.

Supplementary materials related to this article can be found online at doi:10.1016/j.lithos.2011.07.001.

Acknowledgements

We are grateful to discussion with Fang Huang and assistance with the Hf isotope analyses by Jin-Feng Sun and Zhi-Chao Liu. The paper has benefited from review comments of William L. Griffin and another anonymous reviewer and editorial comments of Andrew Kerr. This work was jointly supported by the NSFC (grants 40973044 and 40873045), the grant from the Ministry of Land and Resources of the PRC (No. 200811012) and the Institute of Geology and Geophysics, Chinese Academy of Sciences (grant ZC0801).

References

Batumike, J.M., Griffin, W.L., Belousova, E.A., Pearson, N.J., O'Reilly, S.Y., Shee, S.R., 2008. LAM–ICOMS U–Pb dating of kimberlitic perovskite: Eocene–Oligocene kimberlites from the Kundelungu Plateau, D. R. Congo. Earth and Planetary Science Letters 267, 609–619.

Belousova, E.A., Griffin, W.L., Shee, S.R., Jackson, S.E., O'Reilly, S.Y., 2001. Two age populations of zircons from the Timber Creek kimberlites, Northern territory, Australia as determined by laser-ablation ICPMS analysis. Australian Journal of Earth Sciences 48, 757–766.

Chi, J.S., Lu, F.X., 1996. Kimberlites and the Features of Paleozoic Lithospheric Mantle in North China Craton. Science Press, Beijing. 292 pp. (in Chinese with English Summary).

Chu, Z.Y., Wu, F.Y., Walker, R.J., Rudnick, R.L., Pitcher, L., Puchtel, I.S., Yang, Y.H., Wilder, S.A., 2009. Temporal evolution of the lithospheric mantle beneath the eastern North China Craton. Journal of Petrology 50, 1857–1898.

Davis, G.L., Krogh, T.E., Erlank, A.J., 1976. The ages of zircons from kimberlites from South Africa. Year Book—Carnegie Institution of Washington 75, 821–824.

Deng, J.F., Su, S.G., Niu, Y.L., Liu, C., Zhao, G.C., Zhao, X.G., Zhou, S., Xu, Z.X., 2007. A possible model for the lithospheric thinning of North China Craton: evidence from the Yanshanian (Jura-Cretaceous) magmatism and tectonism. Lithos 96, 22–35.

Dobbs, P.N., Duncan, D.J., Hu, S., Shee, S.R., Colgan, E.A., Brown, M.A., Smith, C.B., Allsopp, H.P., 1994. The Geology of Mengyin Kimberlites, Shandong, China. In: Meyer, O.A., Leonardos, O.H., Gaspar, J.C. (Eds.), Kimberlites, Related Rocks and Mantle Xenoliths. Proceedings of the 5th International Kimberlite Conference, Araxá, Brazil, 1991: Companhia de Pesquisa de Recursos Minerais–CPRM Special Publication, Brasilia, 1A/93, pp. 40–61.

Dong, Z.X., 1994. Kimberlites in China. Science Press, Beijing. (in Chinese with English Abstract) 318 pp.

Fan, W.M., Menzies, M.A., 1992. Destruction of aged lower lithosphere and accretion of asthenosphere mantle beneath eastern China. Geotectonica et Metallogenia 16, 171–180.

Gao, S., Rudnick, R.L., Carlson, R.W., McDonough, W.F., Liu, Y.S., 2002. Re–Os evidence for replacement of ancient mantle lithosphere beneath the North China Craton. Earth and Planetary Science Letters 198, 307–322.

Gao, S., Rudnick, R.L., Yuan, H.-L., Liu, X.-M., Liu, Y.-S., Xu, W.-L., Ling, W.-L., Ayers, J., Wang, X.-C., Wang, Q.-H., 2004. Recycling lower continental crust in the North China Craton. Nature 432, 892–897.

Gao, S., Rudnick, R.L., Xu, W.-L., Yuan, H.-L., Liu, Y.-S., Walker, R.J., Puchtel, I.S., Liu, X., Huang, H., Wang, X.-R., Yang, J., 2008. Recycling deep cratonic lithosphere and generation of intraplate magmatism in the North China Craton. Earth and Planetary Science Letters 270, 41–53.

Griffin, W.L., Zhang, A.D., O'Reilly, S.Y., Ryan, G., 1998. Phanerozoic evolution of the lithosphere beneath the Sino-Korean Craton. In: Flower, M., Chung, S.L., Lo, C.H., Lee, T.Y. (Eds.), Mantle dynamics and plate interactions in East Asia. : Geodynamic Series, vol. 27. American Geophysical Union, Washington D.C., pp. 107–126.

Griffin, W.L., Pearson, N.J., Belousova, E., Jackson, S.E., van Achterbergh, E., O'Reilly, S.Y., Shee, S.R., 2000. The Hf isotope composition of cratonic mantle: LAM-MC-ICPMS analysis of zircon megacrysts in kimberlites. Geochimica et Cosmochimica Acta 64, 133–147.

Heaman, L.M., 1989. The nature of the subcontinental mantle from Sr–Nd–Pb isotopic studies on kimberlitic perovskite. Earth and Planetary Science Letters 92, 323–334.

Heaman, L.M., LeCheminant, A.N., 1993. Paragenesis and U–Pb systematics of baddeleyite (ZrO_2). Chemical Geology 110, 95–126.

Heaman, L.M., LeCheminant, A.N., 2000. Anomalous U–Pb systematics in mantle-derived baddeleyite xenocrysts from Île Bizard: evidence for high temperature radon diffusion? Chemical Geology 172, 77–93.

Huang, F., Li, S.G., Yang, W., 2007. Contributions of the lower crust to Mesozoic mantle derived mafic rocks from the North China Craton: implications for lithospheric thinning. In: Zhai, M.G., Windley, B.F., Kusky, T.M., Meng, Q.R. (Eds.), Mesozoic sub-continental lithospheric thinning under Eastern Asia: Geological Society, London, Special Publications, 280, pp. 55–75.

Kinny, P.D., Compston, W., Bristow, J.W., Williams, I.S., 1989. Archean mantle xenocrysts in a Permian kimberlite: two generations of kimberlitic zircon in Jwaneng DK2, southern Botswana. In: Ross, J. (Ed.), Kimberlites and related rocks: their mantle/crust setting, diamonds and diamond exploration. : Geological Society of Australia Special Publication, vol. 14,(2). Blackwell Scientific Publications, Oxford, pp. 833–842.

Kinny, P.D., Griffin, B.J., Heaman, L.M., Brakhfogel, F.F., Spetsius, Z.V., 1997. SHRIMP U–Pb ages of perovskite from Yakutian kimberlites. Russian Geology and Geophysics 38, 97–105.

Kramers, J.D., Smith, C.B., 1983. A feasibility study of U–Pb and Pb–Pb dating of kimberlites using groundmass mineral fractions and whole-rock samples. Chemical Geology 1, 23–38.

Li, Q.L., Chen, F., Wang, X.L., Li, X.H., Li, C.F., 2005. Ultra-low procedural blank and the single-grain mica Rb-Sr isochron dating. Chinese Science Bulletin 50, 2861–2865.

Li, Q.L., Li, X.H., Liu, Y., Tang, G.Q., 2010a. Precise U–Pb and Pb–Pb dating of Phanerozoic baddeleyite by SIMS with oxygen flooding technique. Journal of Analytical Atomic Spectrometry 25, 1107–1113.

Li, Q.L., Li, X.H., Liu, Y., Wu, F.Y., Yang, J.H., Mitchell, R.H., 2010b. Precise U–Pb and Th–Pb age determination of kimberlitic perovskites by secondary ion mass spectrometry. Chemical Geology 269, 396–405.

Liu, D.Y., Nutman, A.P., Compston, W., Wu, J.S., Shen, Q.H., 1992. Remnants of ≥3800 Ma crust in the Chinese part of the Sino-Korean Craton. Geology 20, 339–342.

Ludwig, K.R., 2003. ISOPLOT 3.00: Geochronological toolkit for Microsoft Excel. Berkeley Geochronology Center Special Publication No. 4, 70 pp.

Ma, X. (Ed.), 1989. Atlas of Active Faults in China. Seismological Press, Beijing, p. 120.

Menzies, M.A., Xu, Y.G., 1998. Geodynamics of the North China Craton. In: Flower, M., Chung, S.L., Lo, C.H., Lee, T.Y. (Eds.), Mantle dynamics and plate interactions in east Asia. : Geodynamic Series, vol. 27. American Geophysical Union, Washington D.C., pp. 155–165.

Menzies, M.A., Fan, W.M., Zhang, M., 1993. Palaeozoic and Cenozoic lithoprobes and the loss of >120 km of Archean lithosphere, Sino-Korean craton, China. In: Prichard, H.M., Alabaster, T., Harris, N.B.W., Neary, V.R. (Eds.), Magmatic processes and plate tectonics: Geological Society, London, Special Publications, 76, pp. 71–78.

Menzies, M.A., Xu, Y.G., Zhang, H.F., Fan, W.M., 2007. Integration of geology, geophysics and geochemistry: a key to understanding the North China Craton. Lithos 96, 1–21.

Mitchell, R.H., 1986. Kimberlites: Mineralogy, Geochemistry, and Petrology. Plenum Press, New York. 442 pp.

Mitchell, R.H., 1995. Kimberlites, Orangites, and Related Rocks. Plenum Press, New York. 410 pp.

Qiu, Z.L., Wu, F.Y., Yu, Q.Y., Xie, L.W., Yang, S.F., 2005. Hf isotopes of zircon megacrysts from the Cenozoic basalts in eastern China. Chinese Science Bulletin 50, 2602–2611.

Rudnick, R.L., Gao, S., Ling, W.L., Liu, Y.S., McDonough, W.F., 2004. Petrology and geochemistry of spinel peridotite xenoliths from Hannuoba and Qixia, North China craton. Lithos 77, 609–637.

Schärer, U., Corfu, F., Demaiffe, D., 1997. U–Pb and Lu–Hf isotopes in baddeleyite and zircon megacrysts from the Mbuji-Mayi kimberlite: constraints on the subcontinental mantle. Chemical Geology 143, 1–16.

Song, B., Nutman, A.P., Liu, D.Y., Wu, J.S., 1996. 3800 to 2500 Ma crustal evolution in the Anshan area of Liaoning Province, northeastern China. Precambrian Research 78, 79–94.

Stacey, J.S., Kramers, J.D., 1975. Approximation of terrestrial lead isotope evolution by a two-stage model. Earth and Planetary Science Letters 26, 207–221.

Steiger, R.H., Jäger, E., 1977. Subcommission on geochronology: convention of the use of decay constants in geo- and cosmochronology. Earth and Planetary Science Letters 36, 359–362.

Wan, G., 1989. The distribution pattern of kimberlites and associated rocks in Shandong, China. In: Ross, J. (Ed.), Proceedings of the Fourth International Kimberlite Conference, v. 1, Kimberlites and Related Rocks: Their Composition, Occurrence, Origin and Emplacement. Geological Society of Australia Special Publication, vol.14. Blackwell Scientific Publications, Oxford, pp. 401–406.

Williams, I.S., Hergt, J.M., 2000. U–Pb dating of Tasmanian dolerites: a cautionary tale of SHRIMP analysis of high U zircon. In: Woodhead, J.D., Hergt, J.M., Nobel, W.P. (Eds.), Beyond 2000: new frontiers in isotope geosciences: Abstract and Proceedings, pp. 185–188.

Wingate, M.T.D., Compston, W., 2000. Crystal orientation effects during ion microprobe U–Pb analysis of baddeleyite. Chemical Geology 168, 75–97.

Woolley, A.R., Bergman, S., Edgar, A.D., Le Bas, M.J., Mitchell, R.H., Rock, N.M.S., Scott Smith, B.H., 1996. Classification of the lamprophyres, lamproites, kimberlites, and the kalsilite-, melilite-, and leucite-bearing rocks. Canadian Mineralogist 34, 175–186.

Wu, F.Y., Walker, R.J., Ren, X.W., Sun, D.Y., Zhou, X.H., 2003. Osmium isotopic constrains on the age of lithospheric mantle beneath northeastern China. Chemical Geology 197, 107–129.

Wu, F.Y., Yang, J.H., Liu, X.M., Li, T.S., Xie, L.W., Yang, Y.H., 2005a. Hf isotopes of the 3.8 Ga zircons in eastern Hebei Province, China: implications for early crustal evolution of the North China Craton. Chinese Science Bulletin 50, 2473–2480.

Wu, F.Y., Zhao, G.C., Wilde, S.A., Sun, D.Y., 2005b. Nd isotopic constraints on the crustal formation of the North China Craton. Journal of Asian Earth Sciences 24, 523–545.

Wu, F.Y., Walker, R.J., Yang, Y.H., Yuan, H.L., Yang, J.H., 2006a. The chemical–temporal evolution of lithospheric mantle underlying the North China Craton. Geochimica et Cosmochimica Acta 70, 5013–5034.

Wu, F.Y., Yang, Y.H., Xie, L.W., Yang, J.H., Xu, P., 2006b. Hf isotopic compositions of the standard zircons and baddeleyites used in U–Pb geochronology. Chemical Geology 234, 105–126.

Wu, F.Y., Zhang, Y.B., Yang, J.H., Xie, L.W., Yang, Y.H., 2008a. Zircon U–Pb and Hf isotopic constraints on the Early Archean crustal evolution in Anshan of the North China Craton. Precambrian Research 167, 339–362.

Wu, F.Y., Xu, Y.G., Gao, S., Zheng, J.P., 2008b. Lithospheric thinning and destruction of the North China Craton. Acta Petrologica Sinica 24, 1145–1174 (in Chinese with English abstract).

Wu, F.Y., Yang, Y.H., Marks, M., Liu, Z.C., Zhou, Q., Ge, W.C., Yang, J.S., Zhao, Z.F., Mitchell, R.H., Markl, G., 2010. *In situ* U–Pb, Sr, Nd, and Hf isotopic analysis of eudialyte by LA-(MC)-ICP-MS. Chemical Geology 273, 8–34.

Xu, Y.G., 2001. Thermo-tectonic destruction of the Archean lithospheric keel beneath eastern China: evidence, timing and mechanism. Physics and Chemistry of the Earth (A) 26, 747–757.

Xu, W.L., Hergt, J.M., Gao, S., Pei, F.P., Wang, W., Yan, D.P., 2008. Interaction of adakitic melt-peridotite: implications for the high-Mg# signature of Mesozoic adakitic rocks in the eastern North China Craton. Earth and Planetary Science Letters 265, 123–137.

Yang, Y.H., Wu, F.Y., Wilde, S.A., Liu, X.M., Zhang, Y.B., Xie, L.W., Yang, J.H., 2009. In situ perovskite Sr–Nd–Hf isotopic constraints on the petrogenesis of the Ordovician Mengyin Kimberlites in the North China Craton. Chemical Geology 264, 24–42.

Yin, Z.W., Lu, F.X., Chen, M.H., 2005. SHRIMP age of exotic zircons in the Mengyin kimberlite, Shandong, and their formation. Acta Geologica Sinica 79, 654–661.

Ying, J.F., Zhang, H.F., Sun, M., Tang, Y.J., Zhou, X.H., Liu, X.M., 2007. Petrology and geochemistry of Zijinshan alkaline intrusive complex in Shanxi Province, western North China Craton: implication for magma mixing of different sources in an extensional regime. Lithos 98, 45–66.

Zhang, H.F., 2005. Transformation of lithospheric mantle through peridotite-melt reaction: a case of Sino-Korean craton. Earth and Planetary Science Letters 237, 768–780.

Zhang, H.F., Yang, Y.H., 2007. Emplacement age and Sr–Nd–Hf isotopic characteristics of the diamondiferous kimberlites from the eastern North China Craton. Acta Petrologica Sinica 23, 285–294 (in Chinese with English abstract).

Zhang, P., Hu, S., Wan, G., 1989. The distribution pattern of kimberlites and associated rocks in Shandong, China. In: Ross, J. (Ed.), Proceedings of the Fourth International Kimberlite Conference, v. 1, Kimberlites and related rocks: their composition, occurrence, origin and emplacement. : Geological Society of Australia Special Publication, vol. 14. Blackwell Scientific Publications, Oxford, pp. 393–400.

Zhang, H.F., Goldstein, S.L., Zhou, X.H., Sun, M., Zheng, J.P., Cai, Y., 2008. Evolution of subcontinental lithospheric mantle beneath eastern China: Re–Os isotopic evidence from mantle xenoliths in Paleozoic kimberlites and Mesozoic basalts. Contributions to Mineralogy and Petrology 155, 271–293.

Zhang, S.H., Zhao, Y., Yang, Z.Y., He, Z.F., Wu, H., 2009. The 1.35 Ga diabase sills from the northern North China Craton: implications for breakup of the Columbia (Nuna) supercontinent. Earth and Planetary Science Letters 288, 588–600.

Zhao, G.C., Sun, M., Wilde, S.A., Li, S.Z., 2005. Late Archean to Paleoproterozoic evolution of the North China Craton: key issues revisited. Precambrian Research 136, 177–202.

Zheng, J.P., O'Reilly, S.Y., Griffin, W.L., Lu, F.X., Zhang, M., 1998. Nature and evolution of Cenozoic lithospheric mantle beneath Shandong Peninsula, Sino-Korean Craton. International Geology Review 40, 471–499.

Zheng, J.P., Griffin, W.L., O'Reilly, S.Y., Lu, F.X., Wang, C.Y., Zhang, M., Wang, F.Z., Li, H.M., 2004a. 3.6 Ga lower crust in central China: new evidence on the assembly of the North China Craton. Geology 32, 229–232.

Zheng, J.P., Griffin, W.L., O'Reilly, S.Y., Lu, F.X., Yu, C.M., 2004b. U–Pb and Hf–isotope analysis of zircons in mafic xenoliths from Fuxian kimberlites: evolution of the lower crust beneath the North China Craton. Contributions to Mineralogy and Petrology 148, 79–103.

Zheng, J.P., Griffin, W.L., O'Reilly, S.Y., Yang, J.S., Li, T.F., Zhang, M., Zhang, R.Y., Liou, J.G., 2006. Mineral chemistry of peridotites from Paleozoic, Mesozoic and Cenozoic lithosphere: constraints on mantle evolution beneath eastern China. Journal of Petrology 47, 2233–2256.

Zheng, J.P., Griffin, W.L., O'Reilly, S.Y., Yu, C.M., Zhang, H.F., Pearson, N., Zhang, M., 2007. Mechanism and timing of lithospheric modification and replacement beneath the eastern North China Craton: peridotitic xenoliths from the 100 Ma Fuxian basalts and a regional synthesis. Geochimica et Cosmochimica Acta 71, 5203–5225.

Zheng, J.P., Griffin, W.L., O'Reilly, S.Y., Zhao, J.H., Wu, Y.B., Liu, G.L., Pearson, N., Zhang, M., Ma, C.Q., Zhang, Z.H., Yu, C.M., Su, Y.P., Tang, H.Y., 2009. Neoarchean (2.7–2.8 Ga) accretion beneath the North China Craton: U–Pb age, trace elements and Hf isotopes of zircons in diamondiferous kimberlites. Lithos 112, 188–202.